

Optical Engineering

OpticalEngineering.SPIEDigitalLibrary.org

Error-correct arithmetic for angular displacement measurement with single linear image detector

Hai Yu
Qihua Wan
Xinran Lu
Yingcai Du
Changhai Zhao

SPIE.

Hai Yu, Qihua Wan, Xinran Lu, Yingcai Du, Changhai Zhao, "Error-correct arithmetic for angular displacement measurement with single linear image detector," *Opt. Eng.* **57**(5), 054108 (2018), doi: 10.1117/1.OE.57.5.054108.

Error-correct arithmetic for angular displacement measurement with single linear image detector

Hai Yu,* Qiuhua Wan, Xinran Lu, Yingcai Du, and Changhai Zhao

Chinese Academy of Sciences, Changchun Institute of Optics, Fine Mechanics and Physics, Changchun, China

Abstract. This paper proposes a grating eccentricity error correction technique for high-precision angular measurement via image processing. We first built a mathematical model of grating eccentricity error, then we established an error-correct arithmetic based on the least square method. We tested the proposed method to find that it yields a standard error deviation of only 6.33", compared to the uncorrected standard error deviation of 22.33". This method is based on a single detector, which is inexpensive and performs well. The results presented here may provide a theoretical and technological foundation for further research on small-size, high-resolution photographic rotary encoders. © 2018 Society of Photo-Optical Instrumentation Engineers (SPIE) [DOI: 10.1117/1.OE.57.5.054108]

Keywords: angular measurement; error-correct; linear image detector.

Paper 180364 received Mar. 9, 2018; accepted for publication May 2, 2018; published online May 16, 2018.

1 Introduction

It is challenging to achieve high angular measurement precision when grating size is small. When grating diameter is below 40 mm, traditional measurement methods based on moiré fringe can achieve up to 16-bit resolution but no better than 30" precision.¹⁻⁵ Angular measurement-based imaging detectors yield higher resolution and better precision than the traditional moiré fringe method. Advancements in digital image-processing technology⁶⁻¹⁴ have resulted in image detectors highly capable of precise angle measurements, but it is still very challenging to secure high precision with small-size gratings.

Image-type angle measurement technology can be used to distinguish disk reticle images to realize high-resolution and high-precision measurements. In a previous study, we proposed an angular measurement technique¹⁵ capable of high-resolution angular measurement. We also established an arithmetic for dual imaging detectors that minimizes the error caused by grating eccentricity, as shown in Fig. 1. Though the method is effective, the use of two imaging detectors is very costly.

This paper proposes an error-correct arithmetic suited to the use of a single detector. We built a mathematical model for grating eccentricity and determined its parameters by an initial error detection. After we acquired an error function, we used the error-compensation arithmetic to decrease the error caused by grating eccentricity. We conducted an experiment and achieved a standard error deviation of 6.72", compared to an uncorrected standard error deviation of 24.74".

The rest of this paper is organized as follows: Sec. 2 discusses the mathematical model of grating eccentricity error. Section 3 details the proposed error-compensation arithmetic based our analyses of eccentricity. Section 4 presents a series of test results. Conclusions are provided in Sec. 5.

2 Mathematical Model of Eccentricity

A typical grating disk of image type angle measurement is shown in Fig. 2. There are 2^N "reference lines" in a grating disk. Every "reference line" has an equal width.

A and C are two intersections between the linear image detector and "reference lines"; B is the point-intersection between the linear image detector and center line. We used a previously proposed subdivision algorithm¹⁶ to calculate angle displacement as follows:

$$\theta = \frac{2\pi}{2^N} \cdot \frac{BC}{AC}. \quad (1)$$

When the grating is not concentric with the true center, the eccentricity will cause measurement error as shown in Fig. 3.

The center of the grating disk moves from dot O to O' ; θ is the measured angle before moving, θ' is the measured angle after moving; point-intersection A and C move to A' , C' . Eccentricity is marked as P in Fig. 3, where its direction is α . At this time, we calculate angle value θ' by the new point-intersection (A' , C'). According to Eq. (1), the effects of eccentricity on angle displacement calculation can be determined as follows:

$$\theta' = \frac{2\pi}{2^N} \cdot \frac{BC'}{A'C'} = \frac{2\pi}{2^N} \cdot \frac{(BC - P \sin \alpha) \cdot \frac{(BO - P \cos \alpha)}{BO}}{AC \cdot \frac{(BO - P \cos \alpha)}{BO}}. \quad (2)$$

Equation (2) can be rewritten as

$$\theta' = \frac{2\pi}{2^N} \cdot \frac{BC - P \sin \alpha}{AC}. \quad (3)$$

The error between θ and θ' can be calculated as

$$\theta - \theta' = \frac{2\pi}{2^N} \cdot \left(\frac{BC}{AC} - \frac{BC - P \sin \alpha}{AC} \right) = \frac{2\pi}{2^N} \cdot P \sin \alpha, \quad (4)$$

*Address all correspondence to: Hai Yu, E-mail: yuhai@ciomp.ac.cn

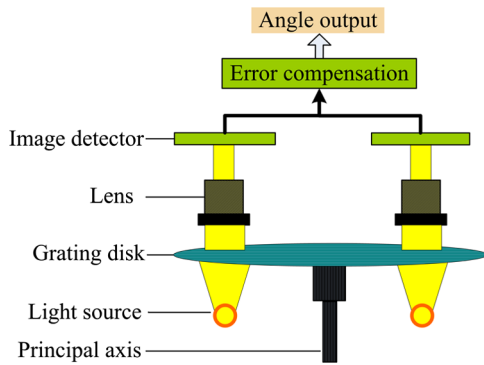


Fig. 1 Compensation principle for two imaging detectors.

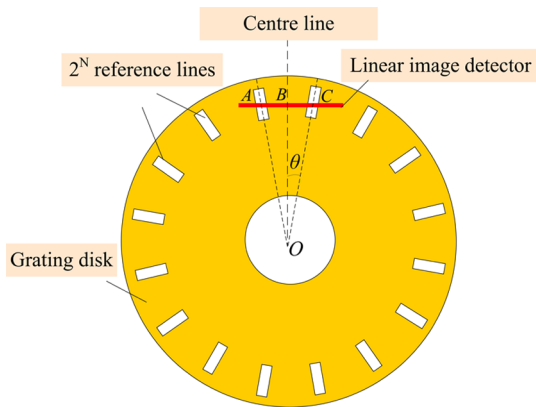


Fig. 2 Typical grating disk of image-type angle measurement.

where error decreases as N increases. In other words, we can decrease eccentricity error by enlarging the grating. In practice, however, the radius of the grating is fixed.

3 Error-Correct Arithmetic

Based on Eq. (4), we wrote the following equation to correct for eccentricity error:

$$f(x) = u \cdot \sin(x - \varphi) + c, \tag{5}$$

where u is the range of error and φ is the phase, c is the offset value.

3.1 Determining Parameters

To determine the parameters, we calibrated the image-type angle measurement device via the “high-precision angle-reference” shown in Fig. 4.

We connected the high-precision angle reference to the image-type angle measurement device coaxially with a coupler and calculated the error according to the difference value. We obtained n error values $f'(x_i) = f'(x_0), f'(x_1), \dots, f'(x_n)$ around the circular device. x_i is the absolute position and a larger n yields a more accurate $f(x)$. We next fit $f'(x_i)$ by Eq. (5), where the difference in square sum between $f(x)$ and $p(x)$ reached a minimum

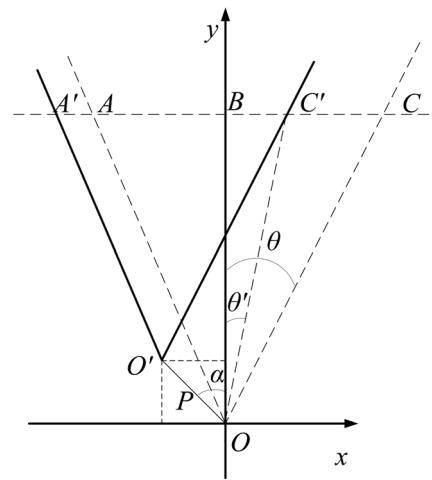


Fig. 3 Grating with eccentricity.

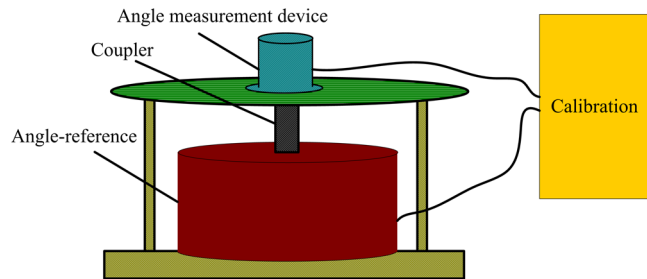


Fig. 4 The principle of errors calibration.

$$F = \sum_{i=0}^n [u \cdot \sin(x_i + \varphi) + c - f'(x_i)]^2. \tag{6}$$

To determine whether F is minimal, we calculated the partial derivatives of u , φ , and c , while letting the partial derivative be zero:

$$\frac{dF}{du} = 2 \sum_{i=0}^n [u \cdot \sin(x_i + \varphi) + c - f'(x_i)] \cdot \sin(x_i + \varphi) = 0, \tag{7}$$

$$\begin{aligned} \frac{dF}{d\varphi} &= 2 \sum_{i=0}^n [u \cdot \sin(x_i + \varphi) + c - f'(x_i)] \cdot u \cdot \cos(x_i + \varphi) \\ &= 0, \end{aligned} \tag{8}$$

$$\frac{dF}{dc} = 2 \sum_{i=0}^n [u \cdot \sin(x_i + \varphi) + c - f'(x_i)] = 0. \tag{9}$$

We could obtain only one group of $\{u, \varphi, c\}$ by this calculation.

3.2 Error-Correct Calculation

Eccentricity error can be corrected after a whole error function is established, as the parameters of the mathematical error model are determined by the initial angle values θ . We changed θ' to binary values and calculated x as

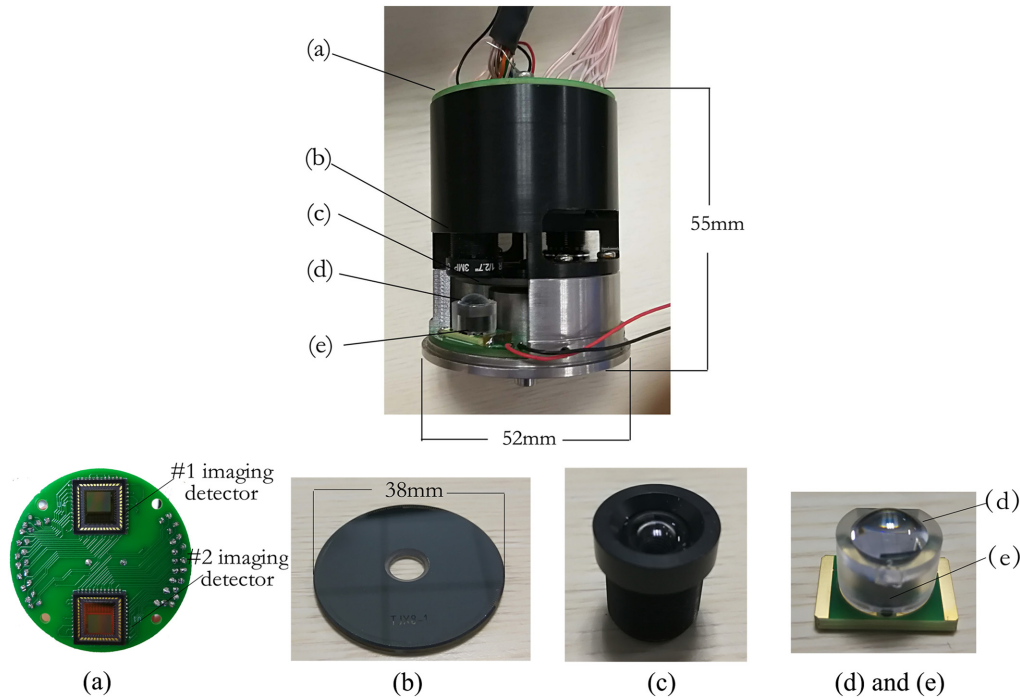


Fig. 5 Test device: (a) circuit, (b) lens, (c) grating disk, (d) lens, and (e) LED (inner).

$$x = \frac{\theta'}{2\pi/2^k}, \tag{10}$$

where $2\pi/2^k$ is the smallest error-correct step. The error-correct arithmetic is as follows:

$$\theta = u \cdot \sin\left(\frac{2\pi}{2^k} \cdot x + \varphi\right) + c + \theta', \tag{11}$$

where $\{u, \varphi, c\}$ has been calculated by Eqs. (7)–(9). The resolution of the error-correct is:

$$r = \left\lfloor \frac{2u}{2^k} \right\rfloor. \tag{12}$$

We set r' as the resolution of the corrected-device in Fig. 4. According to sampling theorem, to ensure the angle output of the corrected device is coherent, the following equation must be met

$$r < \frac{r'}{2}. \tag{13}$$

4 Experiments

We used the angle measurement device described in our previously study to test the proposed arithmetic (Fig. 5). In established setup, parallel light is transmitted across the grating and passes into the lens. The grating patterns are amplified 5× and projected on image detectors. The circuit both collects the pixel-data of the image detector and calculates the angle data via Eq. (3). The grating diameter is $\Phi 38$ mm. There are 2^8 “reference lines” on the circumference of the grating, which achieve subdivision. The resolution of designed device is 21-bit (0.62”).

We used only a single image detector to achieve angle measurement in this study. The grating was deviated revolve-center deliberately as we measured the angle errors of the test device with a 24-polyhedron and autocollimator as shown in Fig. 6. 24-polyhedron is connected to test device by a coupler. We record the errors at each side polyhedron (15 deg). The error before error correction is shown in Fig. 7.

Errors are marked with a blue line in Fig. 7 with a mean square error of 24.74”. There is a one-time sine

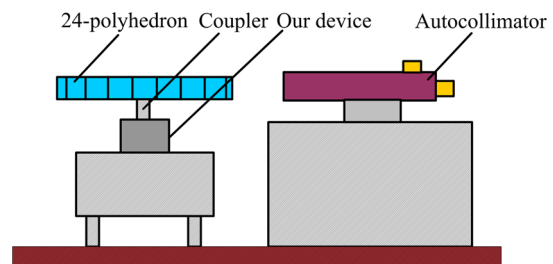


Fig. 6 Error detection.

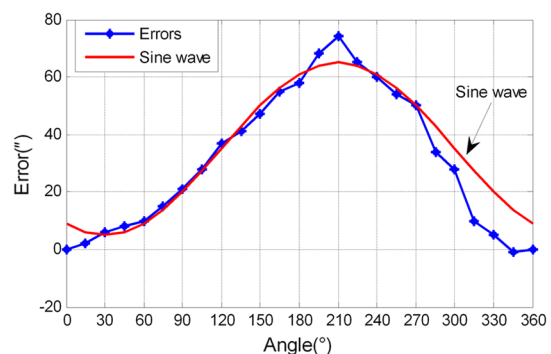


Fig. 7 Error curves before error correction.

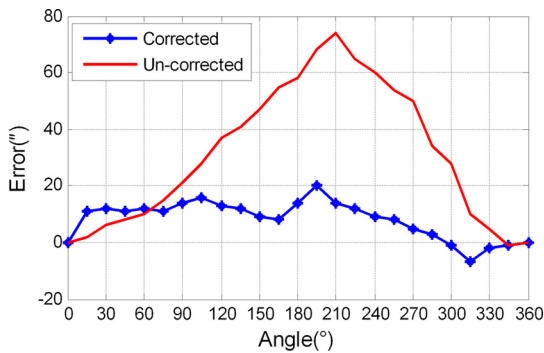


Fig. 8 Error curves after error correction.

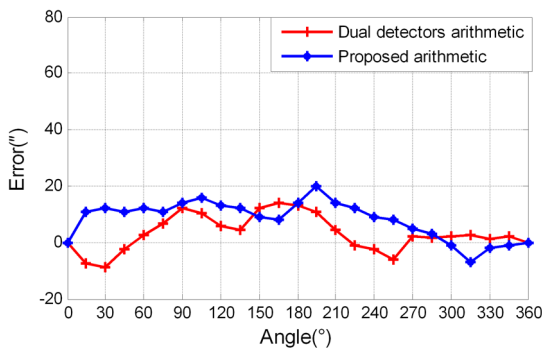


Fig. 9 Error curves of proposed and previously published methods. Mean square error with dual image detectors is 6.33"; that of the proposed arithmetic is 6.72".

wave in this error curve marked with a red line. We fitted the errors by Eq. (5) and obtained the error function $f(x) = -31.2 \sin(x - 0.52) + 34.56$.

To ensure the angle output of the corrected device is coherent, r' must larger than $2r$. In our test, the resolution of designed device is $r' = 0.62''$. By Eq. (12), we set $2^k = 1024$, then $2r = 2 \times (31.2 \times 2/1024) = 0.12$, satisfied Eq. (13). So, we did error correction in our device; the resulting error curve is shown in Fig. 8.

Errors are marked by a blue line in Fig. 8 where the mean square error is 6.72". The precision was better after error correction and eccentricity errors decreased. Compared to the test results on a dual image detector from our previously study (red line, Fig. 9), the mean square error is 6.33". The proposed arithmetic yields a marked improvement in precision and only requires a single image detector (blue line, Fig. 9).

5 Conclusions

This paper proposed an effective arithmetic to eliminate eccentricity error based on a single detector. Tests confirmed

that proposed arithmetic markedly decreases eccentricity error. We hope that the results provided here represent a sound technological foundation for small-size angular measurement.

Acknowledgments

We would like to thank the photoelectric displacement sensor group of the Precision Instrument and Equipment R&D Center, Changchun Institute of Optics, Fine Mechanics and Physics, Chinese Academy of Sciences. Funding: This project is supported by Science and Technology Development Programme of Jilin Province (Grant No. 20180520184JH), National Natural Science Foundation of China (Grant No. 51605465).

References

1. K. Hane et al., "A compact optical encoder with micromachined photodetector," *J. Opt. A: Pure Appl. Opt.* **3**, 191 (2001).
2. K. Hane et al., "Integration of grating-image-type encoder using Si micromachining," *Sens. Actuators A* **97**, 139–146 (2002).
3. F. Liu et al., "Error analyses and calibration methods with accelerometers for optical angle encoders in rotational inertial navigation systems," *Appl. Opt.* **52**, 7724–7731 (2013).
4. Q. H. Wan et al., "Design for spaceborne absolute photoelectric encoder of dual numerical system," *Opt. Precis. Eng.* **17**, 52–57 (2009) (In Chinese).
5. F. Deng et al., "Measurement and calibration method for an optical encoder based on adaptive differential evolution-Fourier neural networks," *Meas. Sci. Technol.* **24**, 055007 (2013).
6. A. Luttenberg and F. Perez-Quintán, "Optical encoder based on a non-diffractive beam III," *Appl. Opt.* **48**, 5015–5024 (2009).
7. W. Luo et al., "Pixel super-resolution using wavelength scanning," *Light Sci. Appl.* **5**, e16060 (2016).
8. J. Qin et al., "Deep subwavelength nanometric image reconstruction using Fourier domain optical normalization," *Light Sci. Appl.* **5**, e16038 (2016).
9. S. Witte et al., "Lensless diffractive imaging with ultra-broadband tabletop sources: from infrared to extreme-ultraviolet wavelengths," *Light Sci. Appl.* **3**, e163 (2014).
10. V. J. Cadarso et al., "High-resolution 1D moirés as counterfeit security features," *Light Sci. Appl.* **2**, e86 (2013).
11. A. C. Sobieranski et al., "Portable lensless wide-field microscopy imaging platform based on digital inline holography and multi-frame pixel super-resolution," *Light Sci. Appl.* **4**, e346 (2015).
12. V. Bianco et al., "Quasi noise-free digital holography," *Light Sci. Appl.* **5**, e16142 (2016).
13. Y. Rivenson et al., "Phase recovery and holographic image reconstruction using deep learning in neural networks," *Light Sci. Appl.* **7**, 17141 (2018).
14. F. Y. Yue et al., "High-resolution gray scale image hidden in a laser beam," *Light Sci. Appl.* **7**, 17129 (2018).
15. H. Yu et al., "Small-size, high-resolution angular displacement measurement technology based on imaging detector," *Appl. Opt.* **56**, 755–760 (2017).
16. H. Yu et al., "A robust sub-pixel subdivision algorithm for image-type angular displacement measurement," *Opt. Laser. Eng.* **100**, 234–238 (2018).

Hai Yu is an assistant research fellow, received his doctorate from Changchun Institute of Optics, Fine Mechanics and Physics, Chinese Academy of Sciences in 2014. His research interest has been in the area of electro-optical displacement precision measurement.

Biographies for the authors are not available.